

Accurate Determination of Interfacial Protein Secondary Structure by Combining Interfacial-Sensitive Amide I and Amide III Spectral Signals

Shuji Ye,* Hongchun Li, Weilai Yang, and Yi Luo*

Hefei National Laboratory for Physical Sciences at the Microscale, Department of Chemical Physics, and Synergetic Innovation Center of Quantum Information & Quantum Physics, University of Science and Technology of China, Hefei, Anhui 230026, China

S Supporting Information

ABSTRACT: Accurate determination of protein structures at the interface is essential to understand the nature of interfacial protein interactions, but it can only be done with a few, very limited experimental methods. Here, we demonstrate for the first time that sum frequency generation vibrational spectroscopy can unambiguously differentiate the interfacial protein secondary structures by combining surface-sensitive amide I and amide III spectral signals. This combination offers a powerful tool to directly distinguish random-coil (disordered) and α -helical structures in proteins. From a systematic study on the interactions between several antimicrobial peptides (including LK α 14, mastoparan X, cecropin P1, melittin, and pardaxin) and lipid bilayers, it is found that the spectral profiles of the random-coil and α -helical structures are well separated in the amide III spectra, appearing below and above 1260 cm^{-1} , respectively. For the peptides with a straight backbone chain, the strength ratio for the peaks of the random-coil and α -helical structures shows a distinct linear relationship with the fraction of the disordered structure deduced from independent NMR experiments reported in the literature. It is revealed that increasing the fraction of negatively charged lipids can induce a conformational change of pardaxin from random-coil to α -helical structures. This experimental protocol can be employed for determining the interfacial protein secondary structures and dynamics in situ and in real time without extraneous labels.

Structure determination holds the key for understanding and controlling the functionality of biological systems. With very limited tools at hand, there is an ever-growing demand for new and better experimental methods to accurately determine the structures—particularly the interfacial structures—of the proteins. The lack of surface-sensitive and label-free techniques has made it virtually impossible to explicitly distinguish the interfacial protein secondary structures. Consequently, many scientific problems that are associated with the identification of protein structures at the interface remain elusive. Precise molecular details of the interfacial protein structures are not only of scientific interest but also essential for the development of novel biomaterials¹ and for finding effective treatments for “protein deposition diseases” such as Alzheimer’s, Parkinson’s, and prion diseases.² These diseases are known to originate from

the conformational transition of proteins at the interface. In this study, we carefully examine the relevance of surface-sensitive sum frequency generation vibrational spectroscopy (SFG-VS) for the determination of interfacial protein secondary structures. An experimental protocol that combines amide I and amide III spectral signals is successfully developed to accurately differentiate random-coil and α -helical structures at the interface.

SFG-VS, a second-order coherent optical technique, was already developed into a powerful and versatile tool to identify interfacial molecular species (or chemical groups) and to provide information on the orientation of functional groups at a surface or an interface in situ and in real time.³ This technique was successfully applied to characterize the structures and orientation of peptides and proteins in different chemical environments by probing backbone amide I vibration.⁴ The backbone vibrations of proteins are known as the amide vibrations in three different energy regions of amide I, II, and III. Although all amide frequencies are conformation-sensitive, the amide I vibration is the only one that has been used for secondary-structure analysis in previous SFG studies, mainly for two reasons: (1) The amide I vibration (arising mainly from the C=O stretching vibration with minor contributions from the out-of-phase C–N stretching vibration) depends on the secondary structure of the backbone and is hardly affected by the nature of the side chains.⁵ (2) The signals of amides II and III are too weak to be detected. However, there is a strong overlap between amide I signals and the water bending modes at $\sim 1645 \text{ cm}^{-1}$. Infrared energy loss due to the absorption of water vapor from the atmosphere can introduce some errors and uncertainties in the interpretation of SFG-VS results.⁶ The biggest drawback is that the characteristic amide I bands of various secondary structures are clustered in the spectral region of 1600–1700 cm^{-1} . It becomes extremely difficult, if not impossible, to distinguish α -helical and random-coil structures because of the overlap of their frequencies at $\sim 1655 \text{ cm}^{-1}$.^{4c} Consequently, the structural information deduced from SFG amide I signals often differs from that determined by well-established nuclear magnetic resonance (NMR) and circular dichroism (CD) experiments.

The difficulties associated with amide I bands can, in principle, be completely removed when amide III bands (between 1200 and 1400 cm^{-1}) are considered. An introduction to amide III bands is given in the Supporting Information (SI). In general,

Received: October 30, 2013

Published: January 2, 2014

there is no water interference in this region. The so-called amide III₃ band (denoted as amide III below) is predominantly the in-phase combination of C–N stretching and N–H in-plane bending vibrations, as revealed by Raman spectroscopy.^{5,7} For different secondary structures of proteins, amide III bands are more resolvable and better defined than amide I bands.⁷ The characterized spectral features of α -helix, β -turn, random coil, and β -sheet are found in the regions of 1260–1310, 1270–1310, 1230–1260, and 1220–1265 cm^{-1} , respectively (Table S1).^{7,8} The amide III frequency is known to be particularly sensitive to the polypeptide backbone conformation due to the coupling of this vibration with $\text{C}\alpha$ –H bending,^{7,9} which depends sensitively on the peptide bond Ramachandran dihedral angle (ψ), the most important parameter for secondary structure changes in peptides/proteins.^{7,9} Furthermore, it is well known that β -sheet structure is the only one active in the amide I SFG spectra with chiral-sensitive polarization combinations (such as psp and spp).^{4,10} It is thus obvious that rich information about the interfacial protein secondary structures will be obtained if the weak amide III signals can be effectively detected and analyzed together with the strong amide I signals under different polarization conditions. Unfortunately, to the best of our knowledge, amide III SFG signals of interfacial proteins have not been measured yet. Here, we report the first successful measurements on amide III SFG spectra of peptides in cell membranes, using several antimicrobial peptides (AMPs) including LK α 14, mastoparan X (MP-X), cecropin P1 (CP-1), pardaxin, and melittin as the models. It is known that the cell lytic activities of AMPs correlate with their secondary structures in membranes as well as with their binding affinity to liposomes.¹¹

We first investigated the secondary structure of LK α 14, a 14-amino acid peptide with the sequence of (LKKLLKL)₂, in negatively charged POPG lipid bilayer by collecting its amide I and III SFG spectra. LK α 14 was chosen because it forms α -helical structure (Figure 1A) in amphiphilic environments.^{4c,d,12} To obtain amide III signals, several technical procedures were employed to enhance the barely measurable SFG signals in this region. The key technical procedures include the use of (1) a near-total internal reflection geometry (Figure S1), (2) a higher voltage to the detector, and (3) a new and longer difference frequency generation crystal to generate a stable IR pulse with energy $>20 \mu\text{J}$. With these improvements, detection of the very weak amide III signals becomes possible for the first time. Figure 1B shows the ssp amide I spectra of LK α 14 in the presence of 20 mM phosphate buffer solution (pH 7.0). The spectra were collected in 2 h after 30 μL of LK α 14 solution (2 mg/mL in DI water) was injected into the phosphate buffer subphase ($\sim 2.0 \text{ mL}$) of the lipid bilayer. The ssp spectra show a strong peak at $\sim 1653 \text{ cm}^{-1}$ and a weak peak at $\sim 1720 \text{ cm}^{-1}$ in POPG lipid bilayer. The 1720 cm^{-1} signal is generated by the carbonyl groups of the lipid bilayer.¹³ The 1653 cm^{-1} peak is an indication of α -

helical structure or random coil structure.⁵ No detectable spp and psp signals allow us to rule out the formation of β -sheet structure. Figure 1C shows the ssp amide III spectra of LK α 14. Neither spp nor ssp signals are observed in the amide III region, while the ssp amide III spectra are dominated by one peak centered at 1275 cm^{-1} . The tilt at the left side is contributed by the symmetric stretching of phosphate group at the lipid head moiety. It is noted that SFG signal from interfacial molecules depends on a property known as the molecular hyperpolarizability tensors $\beta_{lmn}(l,m,n = a,b,c)$, which are the product of the components of the Raman polarizability and IR transition dipole moment.^{3,4} Theoretically, the stretching modes have much larger hyperpolarizability tensors than the bending, wagging, and other deformation modes. Among the bending modes of the common chemical groups, only the one related to the CH_2 bending mode ($\sim 1440 \text{ cm}^{-1}$) has been successfully detected by SFG. No signals from the wagging and other deformation bands were reported yet. This makes it possible for SFG-VS to eliminate the interference of the wagging and other deformation bands in the amide III region that has been problematic for conventional Raman and IR spectra. Hence, the amide III SFG spectra look relatively simpler than Raman spectra. According to Raman spectral features, the 1275 cm^{-1} peak originates from the α -helical structure.^{7,9} Since the amide III band of the random-coil structure locates below 1260 cm^{-1} , we can therefore unambiguously conclude that only α -helical structure contributes to the 1653 cm^{-1} peak, which is in line with the results of NMR, CD, and X-ray photoelectron spectroscopy.^{4c,d,12}

As discussed elsewhere, the protein local secondary structures, as well as the organization of tertiary structures, can be fully determined from the Ramachandran backbone dihedral angles (ϕ, ψ).^{7,9} It has been shown that the amide III frequency is directly correlated to the angle ψ through eq 1,^{7,9c} where T is the temperature (in $^\circ\text{C}$) and the last term accounts for the effect of temperature-dependent hydrogen-bonding to water molecules. A relation between the amide III frequency and ψ is given in Figure S2. The frequency of 1275 cm^{-1} yields an angle of -50° , which matches well with the result of an ideal right-handed α -helix ($\psi = -47^\circ$).^{12a,b}

After obtaining the amide I and III spectra of the peptide with a pure α -helical structure, we turned to investigate the amide I and III spectra of the peptides with varying helicity to demonstrate the superiority of amide III signals in probing interfacial protein structures. The peptides of MP-X, CP-1, pardaxin, and melittin were extensively studied by a number of techniques.^{4,14} Earlier IR and SFG amide I studies indicated that these peptides adopt α -helical structures in cell membrane. However, NMR and CD results suggested that only 50–85% of amino acid residues adopt α -helical structure, and the rest is disordered (Table 1, Figure 2A, and Table S2).^{14,15} For example, the conformation of melittin in phosphatidylcholine vesicles determined by NMR shows two helices at the N (residues 6–10) and C (residues 13–21) termini, while the other residues are disordered.¹⁵ Figure 2B shows the ssp amide I spectra of these peptides in negatively charged lipid bilayer. Accepting the bandwidth difference, the ssp spectra in the amide I region are all dominated by a single resonance peak centered at 1655 cm^{-1} . No spp or psp signals are observed, indicating that no β -sheet structure is formed. It was suggested that hydrogen/deuterium (H/D) exchange can partially distinguish the random-coil structure from the α -helical

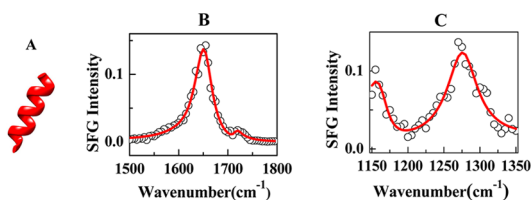


Figure 1. The ssp spectra of LK α 14 in POPG lipid bilayer. (A) Schematics of secondary structures of LK α 14. (B) Amide I spectra. (C) Amide III spectra.

$$\nu_{\text{III}}(\psi) (\text{cm}^{-1}) = 1256 - 54 \sin(\psi + 26^\circ) - 0.11T \quad (1)$$

Table 1. α -Helical Fraction of the Peptides Based on NMR Studies and the Fitting Parameters of Amide III Spectra

peptide	NMR or CD results from the literature		fitting parameters of amide III spectra		
	environment	α -helix fraction (%)	peak 1 (cm^{-1})	peak 2 (cm^{-1})	$\chi_{\text{peak 1}}^{(2)}/\chi_{\text{peak 2}}^{(2)}$
LK α 14	amphiphilic ^{4c,12a}	100	—	1275	0
MP-X	lipid bilayer ^{14a,b}	86	1255	1296	0.217
cecropin P1	phosphatidyl-glycerol ^{14c}	68–88	1237	1297	0.315
	hexafluoro-2-propanol ^{14d}	~77.4			
pardaxin	lipopoly-saccharide ^{14e}	~63.6	1228	1277	0.341
melittin	phospholipid ^{14f,15}	~54	1227	1283	0.582

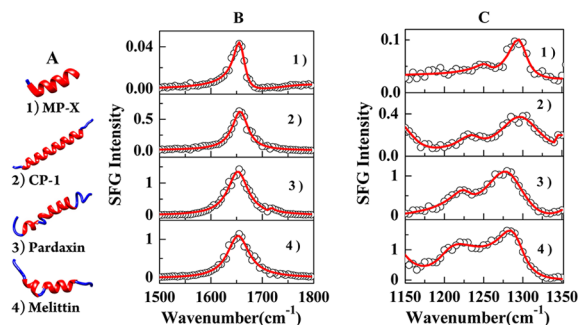


Figure 2. The ssp amide spectra of the peptides of (1) MP-X, (2) CP-1, (3) pardaxin, and (4) melittin in lipid bilayers. (A) Schematics of secondary structures with red helix and blue random coil given by NMR studies.^{14,15} (B) Amide I spectra. (C) Amide III spectra.

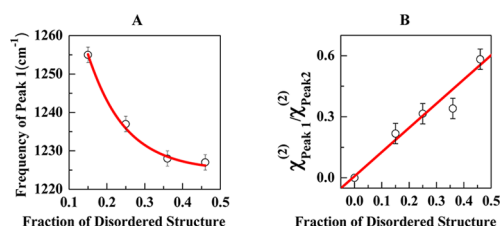


Figure 3. Fitting parameters of the ssp amide III spectra plotted against the fraction of disordered structure: (A) frequency of peak 1 and (B) strength ratio of peaks 1 and 2.

structure because H/D exchange often leads to a larger band shift for the amide I band of the random-coil structure than that of the α -helical structure.⁵ Figure S3 presents the ssp and ppp amide I spectra of DPPG-bilayer-associated melittin in D_2O . It can be seen that the peak center is shifted to 1641 cm^{-1} . Such a large peak shift implies the existence of the random-coil structure. Yet this H/D exchange method does not allow direct identification of the α -helical and random-coil structures.

In contrast to a single peak observed in the amide I region, the amide III spectra (Figure 2C) show two peaks with frequencies below (“peak 1”) and above (“peak 2”) 1260 cm^{-1} , respectively. No amide III signals are detected in ssp and psp spectra. The frequency of peak 2 of LK α 14, pardaxin, and melittin falls in the range of $1280 \pm 5 \text{ cm}^{-1}$, whereas it blue-shifts to $\sim 1295 \text{ cm}^{-1}$ for MP-X and CP-1. The signals in the $1200\text{--}1300 \text{ cm}^{-1}$ range have been confirmed to originate from the backbone amide III vibration rather than the side chains of peptides or lipid molecules. A detailed discussion is given in the SI (Figures S4–S10). The amide I spectra of these peptides were well studied by FTIR and Raman spectroscopy; however, the amide III spectra were sparsely investigated. Recently, Kim et al. reported the amide III spectra of melittin and cecropin A in buffer and different lipid environments using UV resonance Raman spectra.¹⁶ Two peaks centered at ~ 1243 and 1292 cm^{-1} were

observed in the Raman spectra and assigned to the random-coil and α -helical structures, respectively. Accordingly, peaks 1 and 2 in the SFG spectra should originate from random-coil and α -helical structures.

To qualitatively analyze the random-coil and α -helical structure, we fitted the spectra in Figure 2C using a standard procedure (see eq S2). The fitted peak center and strength ratio of peaks 1 and 2 are presented in Table 1. The ratios of peaks 1 and 2 in both ssp and ppp spectra are almost the same (Figure S11, Table S3). The ψ angle determined for melittin molecules ($\psi = -59^\circ$) is very close to the NMR results ($\psi = -60^\circ$).¹⁵ In Figure 3 we plot the fitting parameters against the fraction of disordered structure given by NMR or CD results in the literature.^{12a,14,15} It is evident that the frequency of peak 1 (Figure 3A) decreases with increasing fraction of disordered structure. A linear correlation between the peak amplitude ratio, $\chi_{\text{peak 1}}^{(2)}/\chi_{\text{peak 2}}^{(2)}$, and the content ratio of the disordered structure is clearly observed (Figure 3B). It is well known that the polarized SFG intensity is determined not only by the surface coverage but also by the orientation and Fresnel coefficients. The results of ppp spectra can rule out the influence of the orientation change. In fact, the disordered structure and α -helical structure of a peptide with a straight backbone chain will have similar averaged orientation angle. Therefore, the linear correlation observed in Figure 3B is possibly due to the fact that the disordered structure and α -helical structure of the studied peptides (with the exception of pardaxin) are arranged along an approximately straight line (Figure 2A). Although melittin has two helices, its disordered structure is also almost in a straight line with its immediately connected α -helical structure (for example, residues 1–5 and residues 6–10). Thus, the ratio $\chi_{\text{peak 1}}^{(2)}/\chi_{\text{peak 2}}^{(2)}$ can be used to roughly characterize the relative content ratio of the disordered and α -helical structures of the peptides with a straight backbone chain, as well as to determine the interfacial conformational transition of the same peptides or proteins. This may open up a new spectral window to address some fundamental problems that cannot currently be tackled using amide I spectra alone. Of course, one needs to mention that such linear correlation may not apply for larger proteins with multiple membrane-spanning domains because the opposite orientation of different domains can result in the cancellation of the SFG signal from the helical structures. Moreover, this linear correlation may not be used for other proteins that contain structures besides the disordered and α -helical structures.

After establishing the above experimental protocol, we then applied this method to determine the interfacial conformational transition in situ by studying the interactions between pardaxin and the mixed DMPC/DMPG lipid bilayers. It has been shown that the pardaxin adopts different structures depending on the membrane charge status.^{14e,17} Figure 4 shows the ssp amide I and III spectra of pardaxin in different lipid bilayers. The center of the dominant peak in the amide I spectra appears at 1655 cm^{-1} when

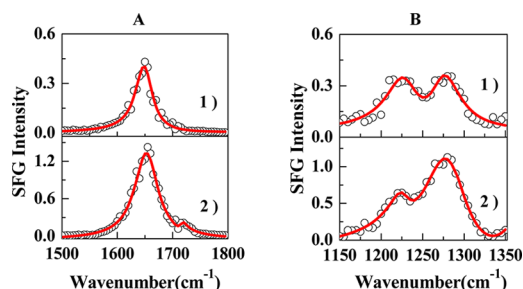


Figure 4. Amide I (A) and amide III (B) ssp spectra of pardaxin in (1) mixed DMPC/DMPG (3/1) bilayer and (2) pure d-DMPG lipid bilayer.

pardaxin interacts with the fully negatively charged d-DMPG bilayer, whereas it red-shifts to 1649 cm^{-1} when pardaxin interacts with the partially negatively charged DMPC/DMPG bilayer (molecular ratio = 3/1) (Figure 4A). The red shift of the peak in mixed DMPC/DMPG bilayers comes from the contribution of the random-coil structure. Consequently, a synchronous change is expected to be observed in the amide III spectra (Figure 4B). The intensity ratio between peak 1 at $\sim 1230\text{ cm}^{-1}$ and peak 2 at $\sim 1280\text{ cm}^{-1}$ ($\chi_{\text{peak 1}}^{(2)}/\chi_{\text{peak 2}}^{(2)}$) increases from 0.34 to 0.73 when the negative charge of the membrane decreases from 100% to 25%. This result indicates that pardaxin undergoes a conformational change from the random-coil structure to the α -helical structure with increasing the fraction of the negatively charged lipids.

Overall, the power and uniqueness of combining SFG amide I and amide III signals to differentiate the interfacial protein secondary structures are convincingly demonstrated in this study. It takes advantage of several superior technical abilities of SFG and some simple spectroscopic characteristics of proteins. For instance, the different combination of polarizations allows us to verify the existence of the β -sheet structure. The well-separated spectral peaks of the random-coil and α -helical structures in the amide III region give direct structural information about the peptides with a straight backbone chain that nicely correlates with information deduced from independent NMR experiments. The possibility to determine the Ramachandran dihedral angles of peptide bonds using the amide III spectra further enriches the knowledge on the local interfacial structure. It is truly remarkable that our method can unambiguously identify the α -helical and random-coil structures for interfacial proteins, resolving an important, long-standing problem in interfacial protein science. It can thus be concluded that our developed method offers a unique and effective optical marker to characterize interfacial protein structures and dynamics.

■ ASSOCIATED CONTENT

Supporting Information

Experimental details, introduction to amide III bands, control experiments, Figures S1–S11, and Tables S1–S4. This material is available free of charge via the Internet at <http://pubs.acs.org>.

■ AUTHOR INFORMATION

Corresponding Authors

shujiye@ustc.edu.cn; yiluo@ustc.edu.cn

Notes

The authors declare no competing financial interest.

■ ACKNOWLEDGMENTS

This work was supported by the National Natural Science Foundation of China (Grants 21073175, 91127042, 20925311, and 21161160557), National Basic Research Program of China (Grant 2010CB923300), and Fundamental Research Funds for the Central Universities (Grant WK2030020023).

■ REFERENCES

- (1) Vallee, A.; Humblot, V.; Pradier, C.-M. *Acc. Chem. Res.* **2010**, *43*, 1297.
- (2) Chiti, F.; Dobson, C. M. *Annu. Rev. Biochem.* **2006**, *75*, 333.
- (3) (a) Shen, Y. R. *The Principles of Nonlinear Optics*; Wiley: New York, 1984. (b) Castellana, E. T.; Cremer, P. S. *Surf. Sci. Rep.* **2006**, *61*, 429.
- (c) Lambert, A.; Davies, P.; Neivandt, D. *Appl. Spectrosc. Rev.* **2005**, *40*, 103. (d) Gopalakrishnan, S.; Liu, D.; Allen, H. C.; Kuo, M.; Shultz, M. J. *Chem. Rev.* **2006**, *106*, 1155. (e) Wang, H.-F.; Gan, W.; Lu, R.; Rao, Y.; Wu, B.-H. *Int. Rev. Phys. Chem.* **2005**, *24*, 191.
- (4) (a) Chen, X.; Wang, J.; Boughton, A. P.; Kristalyn, C. B.; Chen, Z. J. *Am. Chem. Soc.* **2007**, *129*, 1420. (b) Fu, L.; Ma, G.; Yan, E. C. Y. *J. Am. Chem. Soc.* **2010**, *132*, 5405. (c) Fu, L.; Liu, J.; Yan, E. C. Y. *J. Am. Chem. Soc.* **2011**, *133*, 8094. (d) Weidner, T.; Breen, N. F.; Li, K.; Drobny, G. P.; Castner, D. G. *Proc. Natl. Acad. Sci. U.S.A.* **2010**, *107*, 13288. (e) Liu, Y.; Jasensky, J.; Chen, Z. *Langmuir* **2011**, *28*, 2113.
- (5) (a) Barth, A.; Zscherp, C. *Q. Rev. Biophys.* **2002**, *35*, 369. (b) Tamm, L.; Tatulian, S. A. *Q. Rev. Biophys.* **1997**, *30*, 365.
- (6) Vinaykin, M.; Benderskii, A. V. *J. Phys. Chem. Lett.* **2012**, *3*, 3348.
- (7) Oladepo, S. A.; Xiong, K.; Hong, Z. M.; Asher, S. A.; Hander, J.; Lednev, I. K. *Chem. Rev.* **2012**, *112*, 2604.
- (8) (a) Vedantham, G.; Sparks, H. G.; Sane, S. U.; Tzannis, S.; Przybycien, T. M. *Anal. Biochem.* **2000**, *285*, 33. (b) Cooper, E. A.; Knutson, K. *Pharm. Biotechnol.* **1995**, *7*, 101.
- (9) (a) Mix, G.; Schweitzer-Stenner, R.; Asher, S. A. *J. Am. Chem. Soc.* **2000**, *122*, 9028. (b) McColl, I. H.; Blanch, E. W.; Hecht, L.; Kallenbach, N. R.; Barron, L. D. *J. Am. Chem. Soc.* **2004**, *126*, 5076. (c) Mikhonin, A. V.; Bykov, S. V.; Myshakina, N. S.; Asher, S. A. *J. Phys. Chem. B* **2006**, *110*, 1928.
- (10) (a) Wang, J.; Chen, X.; Clarke, M. L.; Chen, Z. *Proc. Natl. Acad. Sci. U.S.A.* **2005**, *102*, 4978. (b) Li, H. C.; Ye, S. J.; Wei, F.; Ma, S. L.; Luo, Y. *Langmuir* **2012**, *28*, 16979.
- (11) (a) Fernández, I.; Ubach, J.; Reig, F.; Andreu, D.; Pons, M. *Biopolymers* **1994**, *34*, 1251. (b) Bechinger, B. *Biochim. Biophys. Acta* **1999**, *1462*, 157.
- (12) (a) DeCrao, W. F.; Lear, J. D. *J. Am. Chem. Soc.* **1985**, *107*, 7684. (b) Drobny, G. P.; Long, J. R.; Karlsson, T.; Shaw, W.; Popham, J.; Oyler, N.; Bower, P.; Stringer, J.; Gregory, D.; Mehta, M.; Stayton, P. S. *Annu. Rev. Phys. Chem.* **2003**, *54*, 531. (c) Bower, P. V.; Oyler, N.; Metha, M.; Long, J. R.; Stayton, P. S.; Drobny, G. P. *J. Am. Chem. Soc.* **1999**, *121*, 8373. (d) Long, J. R.; Oyler, N.; Drobny, G. P.; Stayton, P. S. *J. Am. Chem. Soc.* **2002**, *124*, 6297.
- (13) Ye, S. J.; Li, H. C.; Wei, F.; Jasensky, J.; Boughton, A. P.; Yang, P.; Chen, Z. *J. Am. Chem. Soc.* **2012**, *134*, 6237.
- (14) (a) Whiles, J. A.; Brasseur, R.; Glover, K. J.; Melacini, G.; Komives, E. A.; Vold, R. R. *Biophys. J.* **2001**, *80*, 280. (b) Todokoro, Y.; Yumen, I.; Fukushima, K.; Kang, S. W.; Park, J. S.; Kohno, T.; Wakamatsu, K.; Akutsu, H.; Fujiwara, T. *Biophys. J.* **2006**, *91*, 1368. (c) Gazit, E.; Miller, I. R.; Biggin, P. C.; Sansom, M. S. P.; Shai, Y. *J. Mol. Biol.* **1996**, *258*, 860. (d) Sipos, D.; Andersson, M.; Ehrenberg, A. *Eur. J. Biochem.* **1992**, *209*, 163. (e) Bhunia, A.; Domadia, P. N.; Torres, J.; Hallock, K. J.; Ramamoorthy, A.; Bhattacharjya, S. *J. Biol. Chem.* **2010**, *285*, 3883.
- (f) Dempsey, C. E.; Butler, G. S. *Biochemistry* **1992**, *31*, 11973.
- (15) Okada, A.; Wakamatsu, K.; Miyazawa, T.; Higashijima, T. *Biochemistry* **1994**, *33*, 9438.
- (16) Schlamadinger, D. E.; Wang, Y.; McCammon, J. A.; Kim, J. E. *J. Phys. Chem. B* **2012**, *116*, 10600.
- (17) (a) Vad, B. S.; Bertelsen, K.; Johansen, C. H.; Pedersen, J. M.; Skrydstrup, T.; Nielsen, N. C.; Otzen, D. E. *Biophys. J.* **2010**, *98*, 576. (b) Hallock, K. J.; Lee, D.-K.; Omnaas, J.; Mosberg, H. I.; Ramamoorthy, A. *Biophys. J.* **2002**, *83*, 1004.